Article

Bioleaching of Enargite/Pyrite-rich "Dirty" Concentrate and Arsenic Immobilization

Naoko Okibe [1],*, Kaito Hayashi [1], Keishi Oyama [1], Kazuhiko Shimada [2], Yuji Aoki [3], Takahiro Suwa [3] and Tsuyoshi Hirajima [3]

[1] Department of Earth Resources Engineering, Kyushu University, Fukuoka 819-0395, Japan; k-hayashi19@mine.kyushu-u.ac.jp (K.H.); o.keishi829@gmail.com (K.O.)

[2] Department of Earth and Planetary Sciences, Kyushu University, Fukuoka 819-0395, Japan; kazu@geo.kyushu-u.ac.jp

[3] Sumitomo Metal Mining Co., Ltd., Tokyo 792-0002, Japan; yuji.aoki.m3@smm-g.com (Y.A.); takahiro.suwa.t7@smm-g.com (T.S.); tsuyoshi.hirajima.n7@smm-g.com (T.H.)

* Correspondence: okibe@mine.kyushu-u.ac.jp

Abstract: Bioleaching of arsenic (As)-rich, so-called "dirty" concentrates can produce additional Cu value from the flotation waste while simultaneously releasing toxic As. This study bioleached three such concentrates of varying pyrite/enargite ratios ([Py]/[Ena] = 0.7, 1.3 and 2.4) at a pulp density of 20%. The dissolution behavior of Cu and As in relation to the solution redox potential (Eh) was studied with and without activated carbon (AC) as a potential Eh-controlling catalyst. At this high pulp density, Eh was naturally suppressed, without a need for AC dosing, to <700 mV (a rapid pyrite dissolution is prevented in this Eh range). The effect of AC dosing on Eh varied depending on the type of concentrate; Eh was further reduced only in the case of the most enargite-rich concentrate, DC-I. Among the three concentrates, the highest Cu dissolution (35%) was seen in DC-I (without AC dosing), which simultaneously achieved the lowest As solubilization. Arsenic was immobilized as amorphous precipitates, likely in a mixture of ferric arsenate, cupric arsenate, basic ferric sulfate and sulfur. Arsenic immobilization became increasingly ineffective as the pyrite content increased in the concentrate. Based on these results, setting a lower [Py]/[Ena] ratio prior to the dirty concentrate bioleaching could be a useful approach to promote Cu dissolution and As immobilization simultaneously.

Keywords: enargite; pyrite; concentrate; bioleaching; activated carbon; arsenic immobilization; solution redox potential (Eh); moderately thermophilic acidophiles

1. Introduction

The world's growing metal demand puts further pressure on processing lower-grade, refractory ores with an increasing impurity such as toxic arsenic (As). However, smelters are becoming more selective with the concentrates they buy due to strict environmental regulations, which impose financial penalties for concentrates with excessive As grades [1]. Arsenic-rich, so-called "dirty" concentrates are produced in the flotation process which must be separated from the "clean" concentrates that are brought to the conventional smelting circuit.

Bioleaching can be regarded as one of the promising technologies for scavenging the Cu value from such flotation wastes, from environmental and economic perspectives. One of the representative minerals in dirty concentrates, enargite (Cu_3AsS_4), is an As-bearing, highly refractory primary copper sulfide. Enargite is commonly found in porphyry deposits and high sulfidation epithermal deposits [2,3]. Although detailed descriptions of enargite oxidation in natural environments are scarce, the most common oxidized alteration mineral of enargite is probably scorodite ($FeAsO_4 \cdot 2H_2O$), with Fe provided most likely by pyrite (FeS_2), which is almost ubiquitously associated with enargite [4].

Hence, in dirty concentrates, enargite often co-exists with pyrite as unwanted minerals at varying ratios depending on the original ore composition and flotation process. In hydrometallurgical processing, the dissolution of enargite favors oxidizing conditions (higher *E*h), as with that of pyrite [4]. However, the dissolution of enargite at high *E*h is hindered by that of pyrite, due to the Fe^{3+} mineral passivation on the enargite surface. Consequently, suppressing the *E*h level at around <700 mV is favorable for maintaining steady and longer Cu solubilization from enargite [5–7]. The reason for the need for *E*h control is thus different between enargite and non-As-bearing chalcopyrite ($CuFeS_2$); the latter prefers lower *E*h (~650 mV) to fit into its active leaching state [8–11]. In fact, when bioleaching enargite/chalcopyrite-bearing complex concentrates, the optimal *E*h for maximum Cu leaching increased in response to the increasing enargite/chalcopyrite ratio in the concentrate [6]. During the active bioleaching reaction, the *E*h level can exceed ~800 mV by microbial Fe^{2+} oxidation [5]. In such conditions, the *E*h control through activated carbon (AC)-dosing becomes effective to promote Cu dissolution by preventing rapid pyrite leaching [5]. The AC surface functions as an electron mediator to couple the oxidation of reduced inorganic sulfur compounds (RISCs) and the reduction of Fe^{3+} so that the *E*h level is controlled by offsetting microbial Fe^{2+} oxidation [5].

The solubilization of toxic As is of great concern during the hydrometallurgical processing of dirty concentrates. Therefore, Cu is ideally bioleached selectively from enargite, while As is simultaneously immobilized with the leaching residues. A part of dissolved As(III) is often found to be oxidized and immobilized during bioleaching [12–15]. In thermophilic bioleaching (60–70 °C), enargite is more readily oxidized, and dissolved As can be precipitated as crystalline scorodite [14,16–19]. However, lowering the temperature (such as to 45 °C using moderately thermophilic microorganisms) generally results in slower kinetics in bioleaching, as well as the crystallization of scorodite [20,21]. As the first stage of the biogenic scorodite crystallization process, amorphous As precipitates consisting of ferric arsenate ($FeAsO_4 \cdot nH_2O$) and basic ferric sulfate ($MFe_x(SO_4)_y(OH)_z$) are formed; the dissolution-recrystallization process takes place for phase transformation, wherein SO_4^{2-} ions compete with AsO_4^{3-} to precipitate with Fe^{3+} [19]. In fact, in a bioleaching study of enargite concentrate at 2% pulp density, the loss of *E*h-control led to a sudden initiation of pyrite dissolution (providing SO_4^{2-} ions), which triggered the re-solubilization of ferric arsenate [6].

In this regard, the concept of *E*h-control by AC dosing can serve dual purposes: (i) supporting steady Cu dissolution by preventing rapid pyrite dissolution and (ii) stabilizing As- precipitates, which would otherwise re-solubilize in the bioleaching liquor. While thermophilic bioleaching (60–70 °C) of enargite generally results in high copper dissolutions (52–91%; [12,14,22]), mesophilic bioleaching (25–30 °C) remains to be improved (<15%; [23,24]). In this study using moderately thermophilic microorganisms (45 °C), the bioleaching behavior of three different As-rich dirty concentrates (DC-I, -II and –III at [Py]/[Ena] ratios of 0.7, 1.3 and 2.4, respectively) were compared, especially from the two viewpoints as mentioned above. A high pulp density of 20% (*w/v*) was used to test the feasibility for future practical operation.

2. Materials and Methods

2.1. Characterization of the Concentrates

Three types of high As-content concentrates DC-I (Sumitomo Metal Mining Co., Ltd.; Tokyo, Japan), DC-II (JX Nippon Mining & Metals Co., Ltd.; Tokyo, Japan) and DC-III (Sumitomo Metal Mining Co., Ltd.; Tokyo, Japan), were used in this study (Figure 1). For the elemental analysis, 0.1 g of each concentrate was digested with 5 mL of 35% HCL plus 3 mL of 60% HNO_3 in the microwave digestion system (Ethos Plus, Milestone; Bergamo, Italy) (heated at 1000 W to achieve 230 °C, kept for 15 min, and finally allowed to cool to room temperature). The resultant leachate was filtered (0.45 mm membrane), diluted and measured for concentrations of soluble Cu, Fe and As using inductively coupled plasma-optical emission spectrometry (ICP-OES; Optima 8300, PerkinElmer; Rodgau, Germany). The digestion was performed in duplicate, and the mean metal contents were calculated.

The particle size of the concentrates was measured using a laser diffraction particle size distribution analyzer (Partica LA-950, HORIBA, Kyoto, Japan).
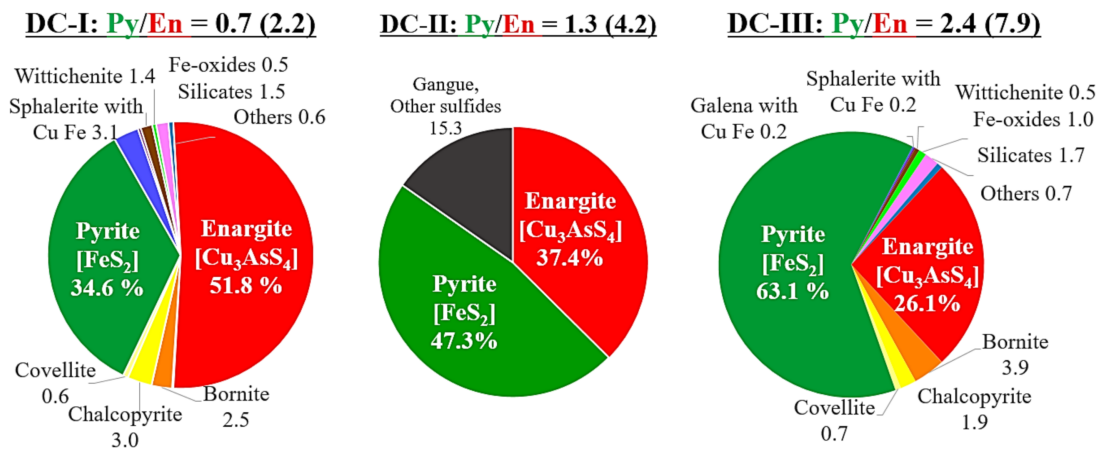
DC-I: Py/En = 0.7 (2.2) **DC-II: Py/En = 1.3 (4.2)** **DC-III: Py/En = 2.4 (7.9)**

DC-I:
- Wittichenite 1.4
- Sphalerite with Cu Fe 3.1
- Fe-oxides 0.5
- Silicates 1.5
- Others 0.6
- Pyrite [FeS$_2$] 34.6 %
- Enargite [Cu$_3$AsS$_4$] 51.8 %
- Covellite 0.6
- Chalcopyrite 3.0
- Bornite 2.5

DC-II:
- Gangue, Other sulfides 15.3
- Enargite [Cu$_3$AsS$_4$] 37.4%
- Pyrite [FeS$_2$] 47.3%

DC-III:
- Sphalerite with Cu Fe 0.2
- Galena with Cu Fe 0.2
- Wittichenite 0.5
- Fe-oxides 1.0
- Silicates 1.7
- Others 0.7
- Pyrite [FeS$_2$] 63.1 %
- Enargite [Cu$_3$AsS$_4$] 26.1%
- Bornite 3.9
- Covellite 0.7
- Chalcopyrite 1.9

Figure 1. The mineral composition (wt %) of three concentrates used in this study (provided by Sumitomo Metal Mining Co., Ltd. for DC-I, III; JX Nippon Mining & Metals Co., Ltd. for DC-II) based on the scanning electron microscope (SEM)-based mineral liberation analysis (MLA). Py/En indicates the weight or molar (in parenthesis) ratio of pyrite/enargite in the concentrates.

2.2. Microorganisms

A mixed culture of six moderately thermophilic, acidophilic microorganisms was prepared and underwent sub-culturing several times on each non-sterilized concentrate, before being used as an inoculum for the bioleaching tests (as described in 2.3.). The six acidophiles inoculated in the mixed culture were: Fe-oxidizing archaeon *Acidiplasma* sp. Fv-Ap, S-oxidizing bacterium *Acidithiobacillus* (*At*.) *caldus* KU (DSM 8584[T]), Fe-oxidizing bacterium *Acidimicrobium* (*Am*.) *ferrooxidans* ICP (DSM 10331[T]), Fe/S-oxidizing bacteria *Sulfobacillus* (*Sb*.) *sibiricus* N1 (DSM 17363[T]), *Sb. thermotolerans* Kr1 (DSM 17362[T]) and *Sb. thermosulfidooxidans* AT-1 (DSM 9293[T]). Sub-cultures were maintained aerobically at 45 °C in acidophile basal salts (ABS) medium (0.5 g/L MgSO$_4$·7H$_2$O, 0.45 g/L (NH$_4$)SO$_4$, 0.15 g/L Na$_2$SO$_4$·10H$_2$O, 0.05 g/L KCl, 0.05 g/L KH$_2$PO$_4$, 0.014 g/L Ca(NO$_3$)$_2$·4H$_2$O; pH$_{ini}$ 1.5 with H$_2$SO$_4$) containing 0.01% yeast extract to support the growth at a high pulp density (20%). Since the mixed culture of *At. caldus* KU, *Am. ferrooxidans* ICP and *Sb. sibiricus* N1 was shown to be effective in the oxidative dissolution of arsenopyrite while releasing over 15 mM total arsenic [15], the three species (plus others available in the laboratory) were used in this study.

2.3. Bioleaching of Dirty Concentrates DC-I, DC-II and DC-III

In our previous bioleaching study on enargite concentrate (at a low pulp density of 2%) using moderately thermophilic microorganisms, the final Cu dissolution was improved from 36% to 53% by dosing 0.2% (*w/v*) of AC. Excessive AC dosing showed an adverse effect (*Eh* too low to leach Cu) [5]. However, since the *Eh* rise tends to slow down at higher pulp densities, especially in As-rich conditions, this study tested a lower AC dosage of 0.025–0.1% (*w/v*).

Bioleaching tests were carried out in 500 mL flasks containing 200 mL ABS media (pH 1.5 with H$_2$SO$_4$) with 0.01% (*w/v*) yeast extract, at a pulp density of 20% (*w/v*) (DC-I, DC-II and DC-III were used as-received, without washing and sterilization). Powdery activated carbon (Shirasagi DO-5; Osaka Gas Chemicals Co. Ltd.; Osaka, Japan; D$_{50}$ = 10.9 μm) was added at different doses (0, 0.025, 0.05 or 0.1%). Pre-grown mixed culture (as described in 2.2) was directly inoculated at 10% (*v/v*) and the flasks were incubated shaken at 150 rpm and 45 °C. All tests were done in duplicate flasks.

Liquid samples were regularly withdrawn to monitor pH, *E*h (vs. SHE), and concentrations of total soluble Cu, As and Fe by ICP-OES. Leaching residues were collected at the end of the bioleaching tests and freeze-dried overnight for X-ray diffraction (XRD; Ultima IV, Rigaku; Tokyo, Japan; CuKα 40mA, 40kV). For quantitative elemental composition analysis by an electron probe microanalyzer (EPMA; JXA-8530F, JEOL; Tokyo, Japan; 6 nA, 20 kV), the leaching residues were embedded into resin and polished. The incident electron beam was focused to 1 μm in diameter and the counting time was set to 20 s for each element. The acquired results were collected by the ZAF method [25].

3. Results and Discussion

3.1. Characterization of Dirty Concentrates

The elemental composition of the concentrates, determined by total acid digestion followed by ICP-OES measurements, is summarized in Table 1 together with their particle sizes. The data listed in Table 1 were mostly consistent with the mineral composition data provided by the companies (Figure 1). The XRD peaks of enargite and pyrite were identified in each concentrate (Figure 2).

Table 1. The elemental composition (based on the total acid digestion analysis) and particle size of each concentrate used in this study.

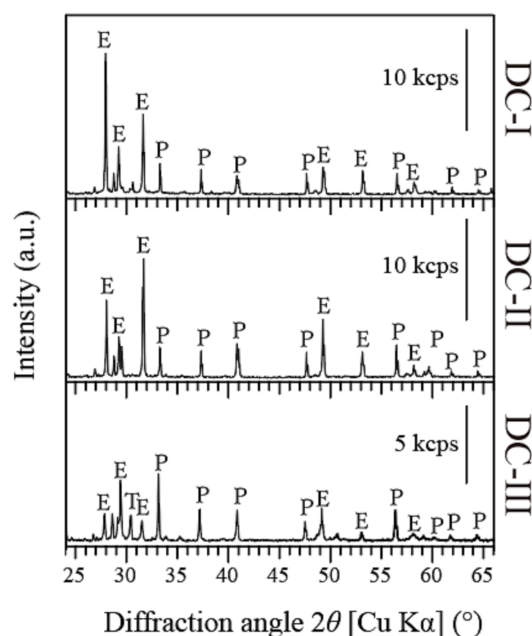| % (*w/w*) (Elemental Ratio Relative to As)	DC-I	DC-II	DC-III
Cu	27.3 ± 0.5% (3.8)	20.4 ± 0.9% (3.7)	14.7 ± 0.2% (3.7)
As	8.5 ± 0.2% (1.0)	6.6 ± 0.4% (1.0)	4.7 ± 0.1% (1.0)
Fe	15.4 ± 0.6% (2.5)	21.2 ± 1.0% (4.3)	29.0 ± 0.6% (8.4)
(As/Cu)	(0.26)	(0.27)	(0.27)
D_{50} (μm)	57.7	62.8	81.2

Figure 2. X-ray diffraction patterns of as-received DC-I, DC-II and DC-III. E: enargite (Cu_3AsS_4; PDF No. 00-035-0775), P: pyrite (FeS_2; PDF No. 00-042-1340), T: tennantite ($Cu_{12}As_4S_{13}$; PDF No. 01-074-1027).

3.2. Bioleaching

In our previous AC bioleaching study on the model chalcopyrite mineral as well as three different chalcopyrite/enargite concentrates at a low pulp density of 1%, the effectiveness of an appropriate amount of AC dosing became particularly evident in suppressing the Eh level to <700 mV, which otherwise rises sharply to >800 mV due to active microbial Fe^{2+} oxidation: the AC's Eh-controlling effect consequently promoted the Cu dissolution from both chalcopyrite and enargite, although for different reasons [6].

On the other hand, a high pulp density of 20% was used in this study. Inoculum-free control tests were conducted for DC-II as a representative concentrate (Figure S1). Without externally added bioleaching microbes, Eh remained too low (~580–615 mV) to promote Cu dissolution (15% at AC 0.05%; 14% at AC 0%; Figure S1). Since all concentrates were used without sterilization (as-received), the results indicate that any possible indigenous microbes did not start a noticeable bioleaching reaction. For DC-I and DC-III, inoculum-free controls were thus omitted. It was already evident during the sub-culturing stage that microbial Fe^{2+}-oxidizing activity was weaker under this As-rich, high pulp density condition (thus, Eh lower). In fact, during the bioleaching period, the Eh level was naturally controlled mostly at <700 mV, even in the AC-free system (Figure 3b,d,f). In this regard, it can be said that the need for AC dosing for the aim of Eh suppression is low as long as bioleaching microbes do not gain full adaptation to such conditions. Generally, pH became more acidic along with the dissolution of more pyrite-rich concentrate (Figure 3b,d,f).
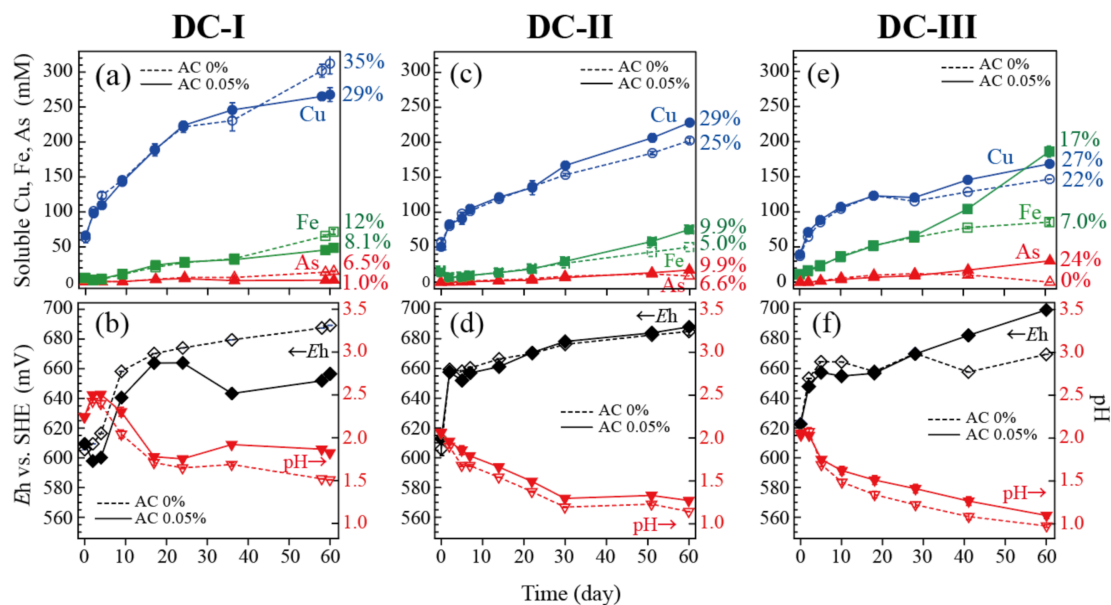

Figure 3. Activated carbon (AC) bioleaching of three concentrates: DC-I (**a**,**b**), DC-II (**c**,**d**) and DC-III (**e**,**f**). Changes in the total soluble Cu (●, ○), Fe (■, □) or As (▲, △) concentration are shown in (**a**,**c**,**e**). Changes in Eh (◆, ◇) and pH (▼, ▽) are shown in (**b**,**d**,**f**). AC was either absent (dotted lines) or added at 0.05% (solid lines). Error bars depicting averages are not visible in some cases as they are smaller than the data point symbols. Percentages marked on the right axis (**a**,**c**,**e**) were calculated as the amount of each soluble metal (on day 60) relative to its content in the concentrate.

Although not shown in Figure 3, three different AC doses (0.025%, 0.05% or 0.1%) were tested but showed nearly identical results. Therefore, only data obtained at AC 0.05% were plotted in Figure 3 for clarity. The effect of AC dosing was seen differently with three concentrates as described in the following:

3.2.1. Concentrate DC-I ([Py]/[Ena] = 0.7)

Although the Eh level in AC-free bioleaching culture was already naturally controlled to <700 mV, the AC dosing further suppressed Eh, especially at the later stage, to around

650 mV (Figure 3b). DC-I had the highest enargite content (Figure 1). Therefore, the Fe^{3+}-reducing effect of AC may have overpowered the microbial Fe^{2+}-oxidizing activity weakened by the higher As toxicity (Figure 3b). Since the enargite mineral itself favors higher *E*h for dissolution (as long as *E*h is kept at <700 mV [5]), the final Cu dissolution from DC-I was greater in the AC-free system (35%) than in the presence of AC (29%) (Figure 3a). Soluble As detected at the end of the bioleaching test was 6.5% (AC-free) or 1.0% (AC 0.05%) (Figure 3a). Since enargite (Cu_3AsS_4) is the dominant Cu mineral in DC-I, which theoretically releases soluble Cu and As at a molar ratio of three, it can be seen that a part of As was immobilized as secondary minerals (Figure 3a), as discussed in 3.3.

3.2.2. Concentrate DC-II ([Py]/[Ena] = 1.3)

Similarly to the case of DC-I, the *E*h level remained max. ~690 mV even without AC. In the case of DC-II, however, AC dosing did not further reduce *E*h (Figure 3d). As a result, all parameters behaved in a rather similar way regardless of the AC dosing (Figure 3c,d). This difference between DC-I and DC-II may have arisen from the higher As content in the former, which provided harsher conditions for microbes to maintain the *E*h level. The Cu dissolution was only slightly higher with AC (29%) than without AC (25%), in response to a slight difference in the *E*h level between the two (Figure 3c,d). Again, only a portion of As was detected soluble (9.9% at AC 0.05%; 5.0% at AC 0%; Figure 3c,d), the rest seemingly immobilized with the leaching residue.

3.2.3. Concentrate DC-III ([Py]/[Ena] = 2.4)

Among the three concentrates tested, a unique trend was noticed for DC-III: i.e., even though this concentrate had the lowest enargite content, bioleaching microbes seemed to have special difficulties in adapting to it from the sub-culturing stage. Since the As grade of this concentrate was the lowest of all, the observed growth inhibition was likely caused by other factors than As (possibly residual flotation chemicals [26]). This growth inhibitory effect can be seen in Figure 3f, where the *E*h level in the AC-free condition remained relatively low at around 660–670 mV, indicating the weaker microbial Fe^{2+}-oxidizing activity on DC-III, compared to the other two concentrates. However, the AC dosing of DC-III unexpectedly led to *E*h rising to 700 mV (Figure 3f). This observation led to our speculation that AC might exhibit multiple effects depending on the condition: i.e., (i) AC's *E*h-suppressing effect emerges when its chemical Fe^{3+}-reducing effect overcomes microbial Fe^{2+} oxidation such as in high-As-grade conditions; (ii) On the other hand, AC could also function to support microbial growth by absorbing particular growth-inhibitory substances and/or by providing the surface for cell attachment [27]. When pyrite rather than enargite is abundant under the latter situation, *E*h could increase, rather than decrease, in the presence of AC.

This also implied that if such a particular growth-inhibitory factor (hypothetically residual flotation chemicals) did not exist in DC-III, *E*h would have exceeded 700 mV regardless of the AC dosing, due to the abundance of pyrite over enargite in this concentrate. Pyrite itself is generally non-toxic to bioleaching microorganisms and also releases dissolved Fe to cause an *E*h rise during bioleaching. The final Cu dissolution was slightly higher with AC (27%), compared to the AC-free system (22%), as *E*h stayed too low (660–670 mV) for enargite dissolution without AC in the case of this particular concentrate (Figure 3e). Compared to more enargite-rich counterparts, more As (24% with AC) dissolved from DC-III, in accordance with the *E*h-elevation (Figure 3e,f).

The involvement of the galvanic effect between enargite and pyrite is suggested in other studies [28]. However, under the *E*h control of <700 mV, the electromotive force generated between enargite, pyrite and AC was found to be negligible [5]. Therefore, the effect of galvanic interaction is also supposed to be insignificant under the conditions of this study.

3.3. As Immobilization

Should the three concentrates be completely dissolved and all metals remain soluble, the theoretical ratio of soluble As (mM)/Cu (mM) can be calculated to be 0.26 for DC-I or 0.27 for DC-II, -III (Table 1). Compared to these theoretical values, Figure 4 shows actual soluble As/Cu molar ratios as a function of *E*h during the bioleaching. A general trend was found showing that at lower *E*h (<650 mV), the As/Cu ratio remains close to null, whereas the ratio rapidly increases at higher *E*h (Figure 4). This trend became more significant for more pyrite-rich concentrate (DC-III > DC-II > DC-I). In other words, the As immobilization efficiency increased as the concentrate became more enargite-rich when compared at the same *E*h value. For the most enargite-rich DC-I, it was possible to keep the majority of As immobilized during the Cu dissolution (Figure 4).
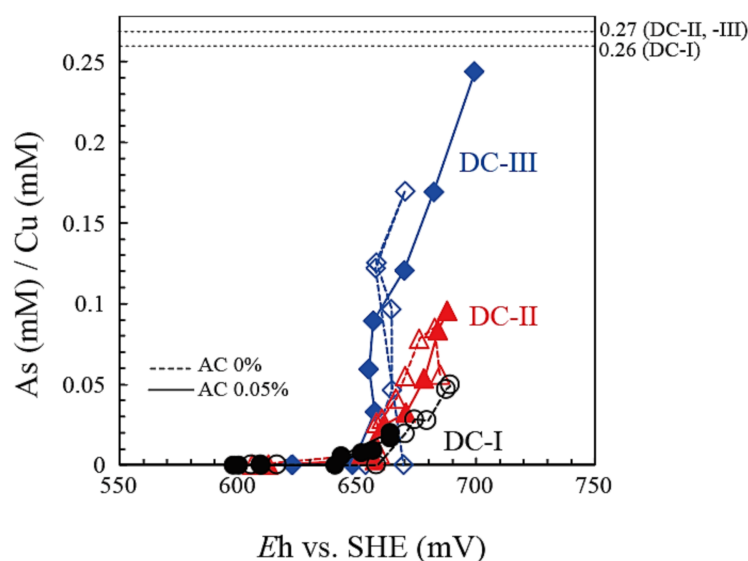

Figure 4. The molar ratio of [soluble As]/[soluble Cu] in the bioleached liquor as a function of *E*h (vs. SHE) during bioleaching of DC-I (●, ○), DC-II (▲, △) and DC-III (◆, ◇) at AC 0% (dotted line) or at AC 0.05% (solid lines). Dotted horizontal lines indicate the theoretical As/Cu ratio upon the complete dissolution of each concentrate based on Table 1.

To understand the form of As immobilization, bioleaching residues were analyzed. Since XRD did not detect any crystalline As-minerals (Figure S2), EPMA analysis was performed. Figure 5 shows larger bioleached DC-I particles together with fine particles of secondary precipitates. The elemental analysis indicates that an enargite-like particle (area 1) is "glued" by aggregated secondary mineral particles composed of As, O, Fe, Cu and S (area 2).

Furthermore, EPMA analysis confirmed that pyrite (with high Fe and S intensities; Figure 6) and enargite grains (with high Cu, As and S intensities) in the bioleached residue were glued within an aggregated matrix composed mainly of Fe, As and O (Figure 6). Table 2 shows further details of the composition of bioleached residues. The brightest particles (7, 9 and 12) are expected to be enargite and less bright particles (1,2,4,5 and 13) pyrite, based on their elemental ratio. Interestingly, the elemental composition of gel-like, dark particles (6, 8 and 12) was very similar to that of finer secondary mineral particles (3, 10 and 14), consisting of As, Fe, Cu and S (some Pb). Therefore, it can be speculated that a number of fine secondary mineral particles may aggregate and transform into larger gel-like particles of a more distinctive form (such as particles 6, 8 and 12). In fact, pieces of such dark gel-like particles can be seen embedded within the fine aggregates all over the image (Table 2).
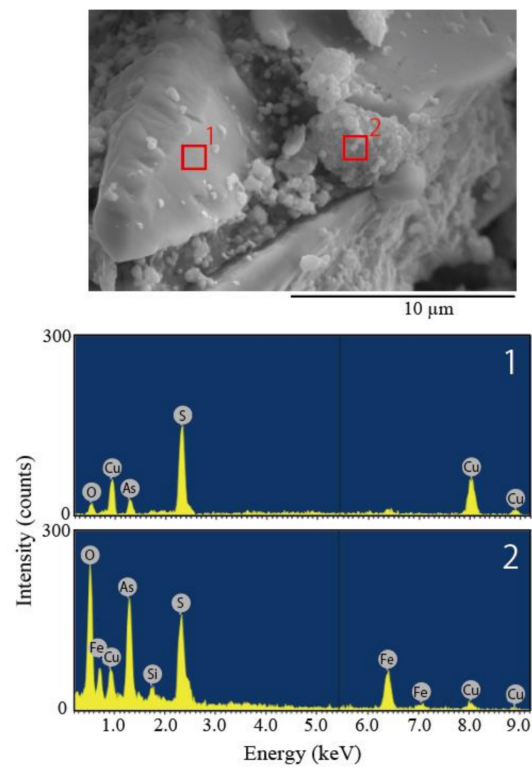
Figure 5. Secondary electron (SE) image and EDS analysis (Oxford Ins. X-act; 15 kV, 5 nA, area analysis mode) of the DC-I residue bioleached for 60 days (without AC).
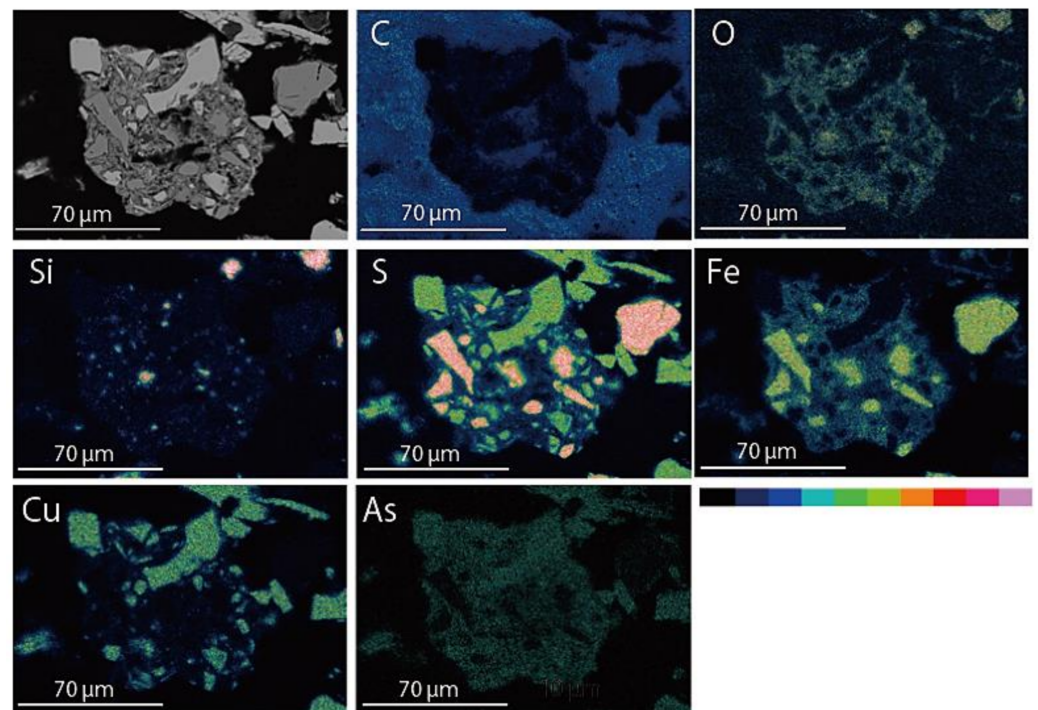

Figure 6. EPMA elemental mapping of DC-II residue bioleached for 60 days at AC 0.05%. The backscattered electron image was mapped for C, O, Si, S, Fe, Cu and As.

Table 2. Backscattered electron image of DC-III residue bioleached for 60 days without AC. Points 1–14 indicate the beam spot positions for the quantitative analysis. Expected mineral types: FeS_2 (no color); Cu_3AsS_4 (grey); secondary As-precipitates (fine particles in light pink; large gel-like particles in dark pink).

No.	S	Sb	Pb	As	Cu	Fe	Zn	Expected Mineral
1	1.8	0	0	0	0	1.0	0	FeS_2
2	2.0	0	0	0	0	1.0	0	FeS_2
3	1.3	0	0.2	1.0	0.5	1.5	0	Secondary precipitates
4	2.1	0	0	0	0	1.0	0	FeS_2
5	2.0	0	0	0	0	1.0	0	FeS_2
6	1.9	0	0.1	1.0	0.4	1.2	0	Secondary precipitates
7	2.8	0.2	0	1.0	2.4	0.3	0.3	Cu_3AsS_4
8	1.8	0	0.1	1.0	0.7	1.1	0	Secondary precipitates
9	3.9	0.2	0	1.0	3.1	0.6	0.2	Cu_3AsS_4
10	5.5	0	0	1.0	0.4	4.3	0	Secondary precipitates
11	5.9	0	0	1.0	0.5	4.6	0	Secondary precipitates
12	4	0.1	0	1.0	3	0.2	0.0	Cu_3AsS_4
13	2.1	0	0	0	0	1.0	0	FeS_2
14	13	0	0	1.0	0.4	6.9	0	Secondary precipitates

10 μm
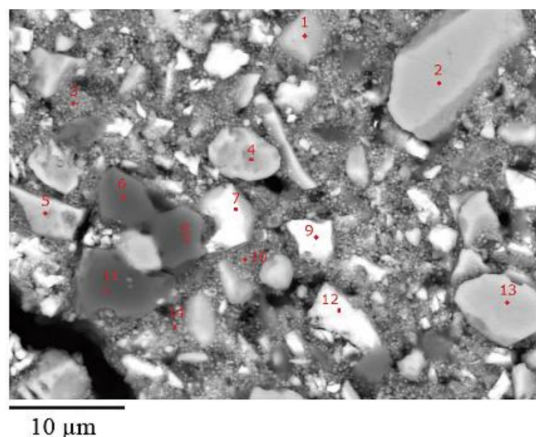
Based on the elemental composition analysis in Table 2, the secondary precipitates can be a mixture of several amorphous minerals such as ferric arsenate, cupric arsenate, basic ferric sulfate and elemental sulfur. Under the moderately thermophilic temperature (45 °C) used in this study, the kinetics of As mineral crystallization is generally slow and amorphous precipitates are readily formed [20,21]. As described by Tanaka et al. [16], the initial amorphous precursor during the scorodite formation process consists of ferric arsenate ($FeAsO_4 \cdot nH_2O$) and basic ferric sulfate ($MFe_x(SO_4)_y(OH)_z$), which gradually transform to crystalline phase under a higher temperature of 70 °C. The formation of both scorodite and cupric arsenate is also suggested in the actual enargite bioleaching test at 70 °C [12]. Since SO_4^{2-} competes with AsO_4^{3-} to precipitate with Fe^{3+} as an amorphous phase [16], As immobilization is thought to become harder in the bioleaching of more pyrite-rich concentrates which provide more SO_4^{2-} ions in the system (Figure 4). Therefore, it can be said that the *E*h level has a significant impact on the As immobilization efficiency; at higher *E*h, where rapid pyrite dissolution initiates, re-solubilization of ferric arsenate is triggered by the shift of chemical equilibrium toward the formation of basic ferric sulfate such as jarosite [19].

Overall, among three types of dirty concentrates with different [Py]/[Ena] ratios, the most enargite-rich DC-I concentrate showed an advantage in terms of Cu dissolution as well as As immobilization. Under the conditions tested this time, AC dosing to the DC-I bioleaching was unnecessary since the *E*h level was naturally suppressed under the As-rich, high pulp density condition. However, where bioleaching microbes are better adapted to such conditions (thus, *E*h exceeds 700 mV), AC dosage may still be a useful approach to adjust the *E*h level. Although further improvement in the Cu dissolution remains, the findings of this study highlight the selective Cu value recoverability from dirty concentrates while leaving most of the As as solids. It was also indicated that pre-adjustment of the [Py]/[Ena] ratio of the dirty concentrate could become a useful approach to realize selective Cu recovery.

4. Conclusions

At a high pulp density of 20%, *E*h was mostly naturally suppressed at <700 mV without the help of the Fe^{3+}-reducing effect of AC, during the bioleaching of three dirty

concentrates. The effect of AC dosing on the *E*h manipulation varied among the three concentrates, depending on their enargite content (and possible inhibitory contaminant): i.e., (i) a further *E*h decrease was noticed for DC-I ([Py]/[Ena] = 0.7); (ii) no effect was observed for DC-II ([Py]/[Ena] = 1.3); or (iii) in contrast, an *E*h increase to >700 mV was seen for DC-III ([Py]/[Ena] = 2.4).

The most enargite-rich DC-I achieved the highest Cu dissolution (35%) while keeping the majority of the As in solid form. The As-immobilization efficiency increased as the [Py]/[Ena] ratio of the concentrate decreased. Arsenic was precipitated as amorphous mixed secondary minerals, likely including ferric arsenate, cupric arsenate, basic ferric sulfate and sulfur. To enhance As immobilization, therefore, the pyrite dissolution should be suppressed to avoid competition between SO_4^{2-} and AsO_4^{3-} to precipitate with Fe^{3+}.

Although further improvement in the Cu dissolution remains, the findings of this study highlight the selective Cu value recoverability from dirty concentrates while keeping most of the As immobilized. It was also indicated that pre-adjustment of the [Py]/[Ena] ratio of the dirty concentrate prior to bioleaching could become a useful approach to realize selective Cu bioleaching.

Supplementary Materials: The following supporting information can be downloaded at: https://www.mdpi.com/article/10.3390/min12040449/s1, Figure S1: Inoculum-free control test for DC-II bioleaching; Figure S2: X-ray diffraction patterns of DC-I (a), DC-II (b) and DC-III (c) before and after bioleaching (with or without AC).

Conflicts of Interest: The authors declare no conflict of interest.

References

1. Long, G.; Peng, Y.; Bradshaw, D. A review of copper–arsenic mineral removal from copper concentrates. *Miner. Eng.* **2012**, *36–38*, 179–186. [CrossRef]
2. Sillitoe, R.H. Porphyry copper systems. *Econ. Geol.* **2010**, *105*, 3–41. [CrossRef]
3. Arribas, A., Jr. Characteristics of high sulfidation epithermal deposits and their relation to magmatic fluid. In *Magmas, Fluids and Ore Deposits*; Thompson, J.F.H., Ed.; Mineralogical Association of Canada Short Course: Ottawa, ON, Canada, 1995; Volume 23, pp. 419–454.
4. Lattanzi, P.; Da Pelo, S.; Musu, E.; Atzei, D.; Elsener, B.; Fantauzzi, M.; Rossi, A. Enargite oxidation: A review. *Earth-Sci. Rev.* **2008**, *86*, 62–88. [CrossRef]
5. Oyama, K.; Shimada, K.; Ishibashi, J.; Sasaki, K.; Miki, H.; Okibe, N. Catalytic mechanism of activated carbon-assisted bioleaching of enargite concentrate. *Hydrometallurgy* **2020**, *196*, 105417. [CrossRef]
6. Oyama, K.; Takamatsu, K.; Hayashi, K.; Aoki, Y.; Kuroiwa, S.; Hirajima, T. Carbon-assisted bioleaching of chalcopyrite and three chalcopyrite/enargite-bearing complex concentrates. *Minerals* **2021**, *11*, 432. [CrossRef]
7. Oyama, K.; Shimada, K.; Ishibashi, J.; Miki, H.; Okibe, N. Silver-catalyzed bioleaching of enargite concentrate using moderately thermophilic microorganisms. *Hydrometallurgy* **2018**, *177*, 197–204. [CrossRef]
8. Gericke, M.; Govender, Y.; Pinches, A. Tank bioleaching of low-grade chalcopyrite concentrates using redox control. *Hydrometallurgy* **2010**, *104*, 414–419. [CrossRef]

9. Masaki, Y.; Hirajima, T.; Sasaki, K.; Miki, H.; Okibe, N. Microbiological redox potential control to improve the efficiency of chalcopyrite bioleaching. *Geomicrobiol. J.* **2018**, *35*, 648–656. [CrossRef]

10. Hiroyoshi, N.; Tsunekawa, M.; Okamoto, H.; Nakayama, R.; Kuroiwa, S. Improved chalcopyrite leaching through optimization of redox potential. *Can. Metall. Q.* **2008**, *47*, 253–258. [CrossRef]

11. Hiroyoshi, N.; Kitagawa, H.; Tsunekawa, M. Effect of solution composition on the optimum redox potential for chalcopyrite leaching in sulfuric acid solutions. *Hydrometallurgy* **2008**, *91*, 144–149. [CrossRef]

12. Escobar, B.; Huenupi, E.; Godoy, I.; Wiertz, J.V. Arsenic precipitation in the bioleaching of enargite by *Sulfolobus* BC at 70 °C. *Biotechnol. Lett.* **2000**, *22*, 205–209. [CrossRef]

13. Sasaki, K.; Takatsugi, K.; Kaneko, K.; Kozai, N.; Ohnuki, T.; Tuovinen, O.H.; Hirajima, T. Characterization of secondary arsenic-bearing precipitates formed in the bioleaching of enargite by *Acidithiobacillus ferrooxidans*. *Hydrometallurgy* **2010**, *104*, 424–431. [CrossRef]

14. Takatsugi, K.; Sasaki, K.; Hirajima, T. Mechanism of the enhancement of bioleaching of copper from enargite by thermophilic iron-oxidizing archaea with the concomitant precipitation of arsenic. *Hydrometallurgy* **2011**, *109*, 90–96. [CrossRef]

15. Tanaka, M.; Yamaji, Y.; Fukano, Y.; Shimada, K.; Ishibashi, J.-I.; Hirajima, T.; Sasaki, K.; Sawada, M.; Okibe, N. Biooxidation of gold-, silver, and antimony-bearing highly refractory polymetallic sulfide concentrates, and its comparison with abiotic pretreatment techniques. *Geomicrobiol. J.* **2015**, *32*, 538–548. [CrossRef]

16. Okibe, N.; Koga, M.; Morishita, S.; Tanaka, M.; Heguri, S.; Asano, S.; Sasaki, K.; Hirajima, T. Microbial formation of crystalline scorodite for treatment of As(III)-bearing copper refinery process solution using *Acidianus brierleyi*. *Hydrometallurgy* **2014**, *143*, 34–41. [CrossRef]

17. Okibe, N.; Morishita, S.; Tanaka, M.; Sasaki, K.; Hirajima, T.; Hatano, K.; Ohata, A. Bioscorodite crystallization using *Acidianus brierleyi*: Effects caused by Cu(II) present in As(III)-bearing copper refinery wastewaters. *Hydrometallurgy* **2017**, *168*, 121–126. [CrossRef]

18. Tanaka, M.; Okibe, N. Factors to enable crystallization of environmentally stable bioscorodite from dilute As(III)-contaminated waters. *Minerals* **2018**, *8*, 23. [CrossRef]

19. Tanaka, M.; Sasaki, K.; Okibe, N. Behavior of sulfate ions during biogenic scorodite crystallization from dilute As(III)-bearing acidic waters. *Hydrometallurgy* **2018**, *180*, 144–152. [CrossRef]

20. Okibe, N.; Nishi, R.; Era, Y.; Sugiyama, T. The effect of heterogeneous seed crystals on arsenite removal as biogenic scorodite. *Mater. Trans.* **2020**, *61*, 387–395. [CrossRef]

21. Okibe, N.; Fukano, Y. Bioremediation of highly toxic arsenic via carbon-fiber-assisted indirect As(III) oxidation by moderately thermophilic, acidophilic Fe-oxidizing bacteria. *Biotechnol. Lett.* **2019**, *41*, 1403–1413. [CrossRef]

22. Muñoz, J.A.; Blázquez, M.L.; González, F.; Ballester, A.; Acevedo, F.; Gentina, J.C.; González, P. Electrochemical study of enargite bioleaching by mesophilic and thermophilic microorganisms. *Hydrometallurgy* **2006**, *84*, 175–186. [CrossRef]

23. Escobar, B.; Huenupi, E.; Wiertz, J.V. Chemical and biological leaching of enargite. *Biotechnol. Lett.* **1997**, *19*, 719–722. [CrossRef]

24. Sasaki, K.; Nakamuta, Y.; Hirajima, T.; Tuovinen, O.H. Raman characterization of secondary minerals formed during chalcopyrite leaching with *Acidithiobacillus ferrooxidans*. *Hydrometallurgy* **2009**, *95*, 153–158. [CrossRef]

25. Boekestein, A.; Stadhouders, A.M.; Stols, A.L.H.; Roomans, G.M. A comparison of ZAF-correction methods in quantitative X-ray microanalysis of light-element specimens. *Ultramicroscopy* **1983**, *12*, 65–68. [CrossRef]

26. Okibe, N.; Johnson, D.B. Toxicity of flotation reagents to moderately thermophilic bioleaching microorganisms. *Biotechnol. Lett.* **2002**, *24*, 2011–2016. [CrossRef]

27. Hao, X.; Liu, X.; Zhu, P.; Chen, A.; Liu, H.; Yin, H.; Qiu, G.; Liang, Y. Carbon material with high specific surface area improves complex copper ores' bioleaching efficiency by mixed moderate thermophiles. *Minerals* **2018**, *8*, 301. [CrossRef]

28. Ma, Y.; Yang, Y.; Gao, X.; Fan, R.; Chen, M. The galvanic effect of pyrite enhanced (bio)leaching of enargite (Cu_3AsS_4). *Hydrometallurgy* **2021**, *202*, 105613. [CrossRef]